Available online at www.sciencedirect.com
ScienceDirect
Journal of Power Sources 175 (2008) 533–539
JOURNAL OF POWER SOURCES
www.elsevier.com/locate/jpowsour

Diphenyloctyl phosphate as a flame-retardant additive in electrolyte for Li-ion batteries

Eun-Gi Shim [a], Tae-Heum Nam [a], Jung-Gu Kim [a,*], Hyun-Soo Kim [b], Seong-In Moon [b]

[a] *Department of Advanced Materials Engineering, Sungkyunkwan University, Suwon 440-746, Republic of Korea*
[b] *Battery Research Group, Korea Electrotechnology Research Institute, Changwon 641-120, Republic of Korea*

Received 20 June 2007; accepted 27 August 2007
Available online 6 September 2007

Abstract

The use of diphenyloctyl phosphate (DPOF) as a flame-retardant additive in liquid electrolyte for Li-ion batteries is investigated. Mesocarbon microbeads (MCMB) and $LiCoO_2$ are used as the anode and cathode materials, respectively. Cyclic voltammetry (CV), differential scanning calorimetry (DSC), electrochemical impedance spectroscopy (EIS), and scanning electron microscopy (SEM) are used for the analyses. The cell with DPOF shows better electrochemical cell performance than that without DPOF in initial charge/discharge and rate performance tests. In cycling tests, a cell with DPOF-containing electrolyte exhibited better discharge capacity and capacity retention than that of the DPOF-free electrolyte after cycling. These results confirm the viability of using DPOF as a flame-retardant additive for improving the cell performance and thermal stability of electrolytes for Li-ion batteries.

Keywords: Lithium-ion battery; Flame retardant; Electrolytes; Diphenyloctyl phosphate; Thermal stability

1. Introduction

Lithium-ion batteries have been successfully used as a power source for portable electric devices such as cellular phones and laptop computers for more than 10 years. Recently, much effort has focused on the development of advanced Li-ion battery technology for use in electric vehicles (EVs) and hybrid electric vehicles (HEVs) [1,2]. Large-scale Li-ion batteries, however, are not yet commercially available for practical applications, due to their associated safety problems.

The electrolyte for Li-ion batteries typically consists of ethylene carbonate (EC), which has a high dielectric constant, and an alkyl carbonate as a low viscosity solvent containing the $LiPF_6$ salt. These solvents are flammable and this could lead to dangerous situations such as leakage, fire and explosion [3,4]. Recently, many researchers have investigated the use of flame-retardant (FR) additives, including trimethyl phosphate (TMP) [5,6], triethyl phosphate (TEP) [5], hexamethyl phosphoramide (HMPA) [7], and 4-isopropyl phenyl diphenyl phosphate (IPPP) [8], to lower the flammability of the liquid electrolytes. Unfortunately, flame retardants have negative effects on the cell performance due to their reactivity with the active materials in Li-ion cells [3]. Xu et al. [9,10] reported that tris(2,2,2-trifluoroethyl) phosphate (TTFP) is a promising flame-retardant additive, which not only reduces the flammability of the liquid electrolyte, but also improves the cycleability of Li-ion cells [9,10].

In the present work, the electrochemical performance of Li-ion cells with and without diphenyloctyl phosphate (DPOF) in ethylene carbonate and ethyl–methyl carbonate (EC:EMC; 3:7 v/v) containing 1.15 M $LiPF_6$ electrolyte is investigated. Differential scanning calorimetry (DSC) is used for thermal stability analysis of the electrolytes, scanning electron microscopy (SEM) for morphological analysis, electrochemical impedance spectroscopy (EIS) for measurement of the resistance change of the cell during cycling, and cyclic voltammetry (CV) for evaluation of the electrochemical stability of the additive-containing electrolytes.

* Corresponding author.
E-mail address: kimjg@skku.ac.kr (J.-G. Kim).

0378-7753/$ – see front matter © 2007 Elsevier B.V. All rights reserved.
doi:10.1016/j.jpowsour.2007.08.098

Table 1
Electrolyte compositions

Electrolyte no.	Composition
E1	1.15 M $LiPF_6$/EC:EMC (3:7 v/v)
E2	1.15 M $LiPF_6$/EC:EMC (3:7 v/v) + DPOF 5% (w/w)

2. Experimental

The charge and discharge tests were performed using 2032 coin-type cells with an electrode diameter of 1.4 cm. The loading of the cathode and anode active materials was about 16.4 and 5.9 mg cm^{-2}, respectively. In the Li-ion cell, mesocarbon microbeads (MCMB) and $LiCoO_2$ were used as the anode and cathode materials, respectively. The electrolyte consisted of 1.15 M $LiPF_6$ dissolved in ethylene carbonate and ethyl–methyl carbonate (EC:EMC; 3:7 v/v). Five weight percent diphenyloctyl phosphate (DPOF) was used as a flame-retardant additive. The compositions of the two different electrolytes are summarized in Table 1. A porous polypropylene film served to separate the anode and cathode. All cells were assembled in a dry room.

The electrochemical stability of the DPOF-containing electrolyte was measured by CV. The CV test was performed using a three-electrode glass cell with an MCMB electrode (2 cm^2) as the working electrode, an $LiCoO_2$ electrode (2 cm^2) as the counter electrode, and a Li foil (1 cm^2) as the reference electrode. The potential was scanned between 0 and 5.5 V versus Li/Li^+ at a scan rate of 1 mV s^{-1}. The CV tests were performed by means of a VMP2 multi-channel potentiostat. The thermal stability of the electrolytes was measured using DSC at a heating rate of 10 °C min^{-1}, in the temperature range from 25 to 350 °C. The DSC measurements were performed using a DSC6200 instrument.

The initial charge/discharge tests of the cells with the two different electrolytes were performed at a rate of 0.1*C*. The rate performance of the cells was measured at rates of 0.2*C*, 0.5*C*, 1*C* and 2*C*. Here, the symbol *C* stands for the current rate provided to cycle the cell system. For example, 0.2*C* means that the charging and discharging processes each take 5 h, i.e., 0.2*C* can be alternatively expressed as a *C*/5 current rate. In the rate performance tests, all of the cells were charged to 4.2 V with a constant current and constant voltage (CC/CV) protocol at a rate of 0.2*C* and then discharged to 2.75 V at different discharge rates. The cycle-life tests were performed using cells with DPOF-free and DPOF-containing electrolytes. The charge and discharge cycling tests were conducted with a VMP2 system at a rate of 1*C* in the voltage range 4.2–2.75 V for 100 cycles. Impedance measurements of the cells during cycling were performed with the same equipment. The frequency was varied from 100 kHz to 10 mHz and the amplitude was set at 10 mV. Impedance data were obtained with ZSimpWin Version 3.00 software. To investigate the morphology on the electrode surface, SEM observation of the samples was performed both before and after cycling.

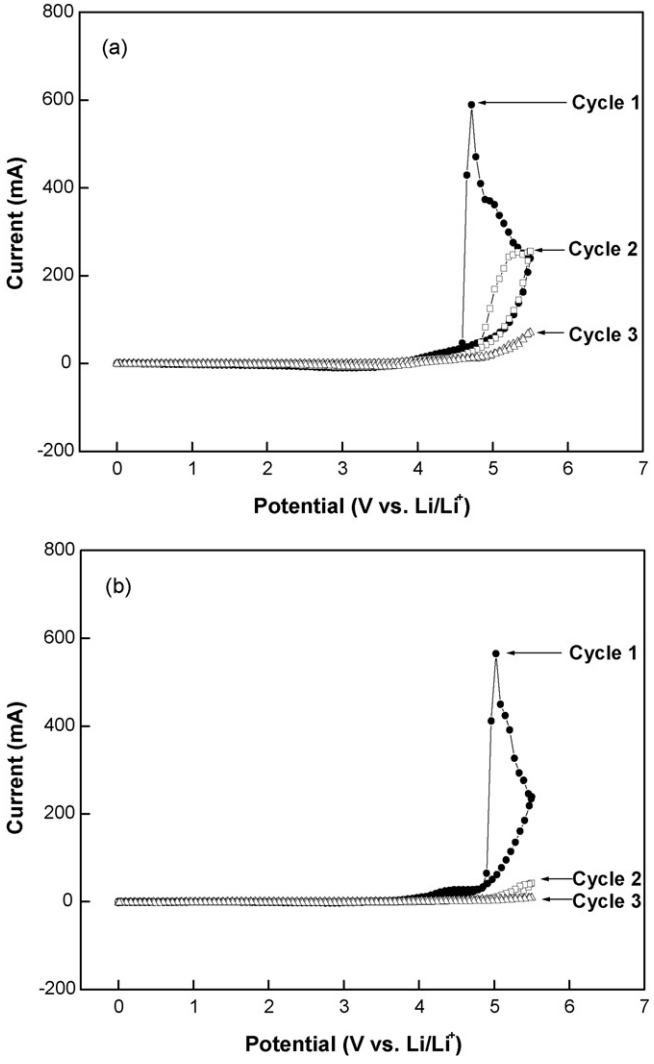

Fig. 1. Cyclic voltammograms of cells consisting of: (a) 1.15 M $LiPF_6$/EC:EMC (3:7 vol.%, reference); (b) reference + DPOF (5 wt.%). Scan rate: 1 mV s^{-1}.

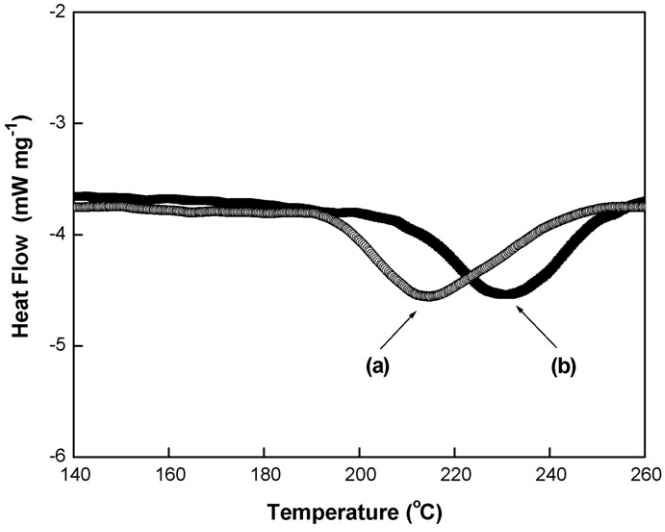

Fig. 2. DSC profiles of electrolytes consisting of: (a) 1.15 M $LiPF_6$/EC:EMC (3:7 vol.%, reference); (b) reference + DPOF (5 wt.%).

Table 2
Irreversible capacity and coulombic efficiency at the first cycle of the cells

Electrolyte no.	Charge capacity (mAh g^{-1})	Discharge capacity (mAh g^{-1})	Irreversible capacity (mAh g^{-1})	Coulombic efficiency (%)
E1	139.6	128.8	10.8	92.3
E2	141.2	132.0	9.2	93.5

3. Results and discussion

To evaluate the electrochemical stability of the DPOF-containing electrolyte, CV tests were carried out in the potential range of 0–5.5 V versus Li/Li^+ using electrolytes with and without DPOF, as shown in Fig. 1. In the DPOF-containing electrolyte, no distinct oxidation peaks are observed up to about 4.95 V versus Li/Li^+. However, the peak of the DPOF-free electrolyte (decomposition at about 4.65 V vs. Li/Li^+) is lower than that of the DPOF-containing electrolyte. Since the working voltage range of the Li-ion cells is 2.5–4.3 V versus Li/Li^+, the results indicate that DPOF can be used as an additive to the electrolyte in Li-ion cells without being oxidized during their normal working voltage range [11,12].

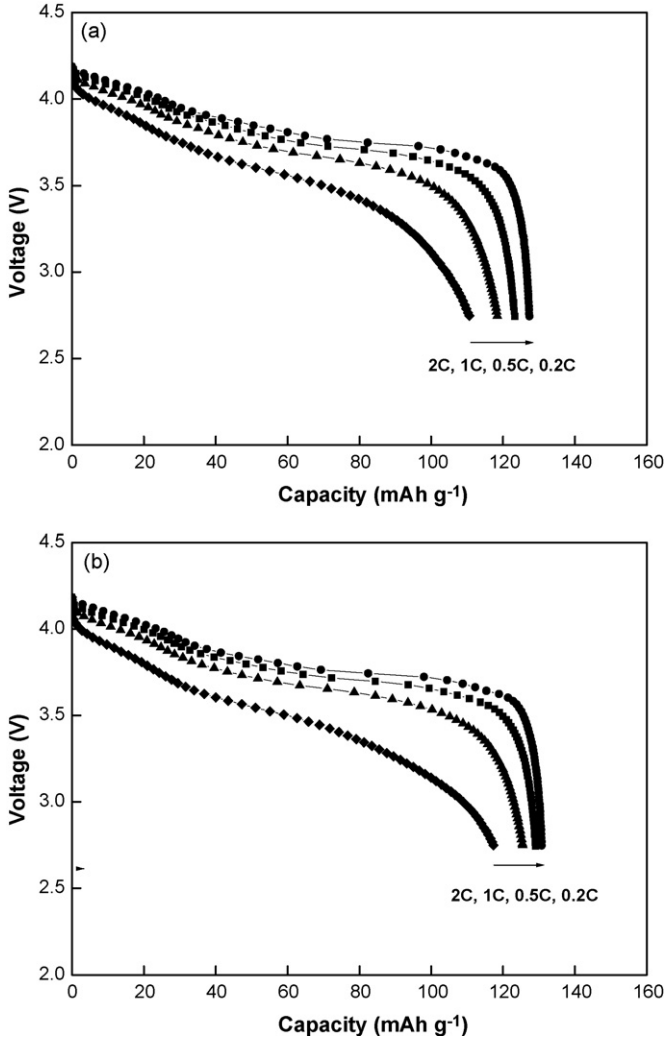

Fig. 3. Discharge capacity of cells at various discharge rates after charging at 0.2*C*: (a) 1.15 M $LiPF_6$/EC:EMC (3:7 vol.%, reference); (b) reference + DPOF (5 wt.%).

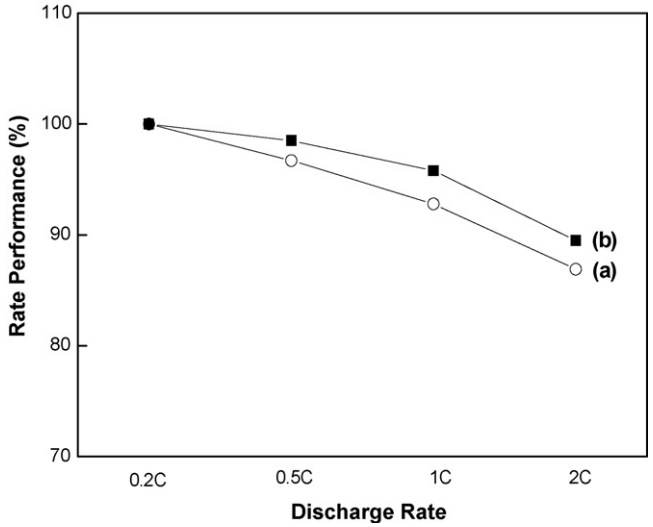

Fig. 4. Rate performance of MCMB/$LiCoO_2$ cells at various discharge rates: (a) 1.15 M $LiPF_6$/EC:EMC (3:7 vol.%, reference); (b) reference + DPOF (5 wt.%).

The DSC curves of electrolytes composed of 1.15 M $LiPF_6$/EC:EMC (3:7 v/v) with and without 5 wt.% DPOF are presented in Fig. 2; the cells are termed E2 and E1, respectively. The reaction peaks are observed at about 231 and 215 °C in electrolytes with and without additive, respectively, confirming the higher thermal stability of the DPOF-containing electrolyte compared with the DPOF-free counterpart.

The initial charge/discharge tests of cells with the two different electrolytes were performed at the 0.1*C* rate. Table 2 presents the charge capacity, discharge capacity, irreversible capacity and coulombic efficiency of these cells. The first discharge capacities of the E1 and E2 cells are 128.8 and 132.0 mAh g^{-1}, while the corresponding irreversible capacities are 10.8 and 9.2 mAh g^{-1}, which produces coulombic efficiencies of 92.3 and 93.5%, respectively. Thus, the cell with the DPOF-containing electrolyte (E2) has a lower irreversible capacity and a better coulombic efficiency. The irreversible capacity may be associ-

Table 3
Rate performance results at various discharge rates in the two different electrolytes

Current rate	Current drains (mA)	Rate performance (%)	
		E1	E2
0.2*C*	0.6	100	100
0.5*C*	1.5	97	99
1.0*C*	3.0	93	96
2.0*C*	6.0	87	90

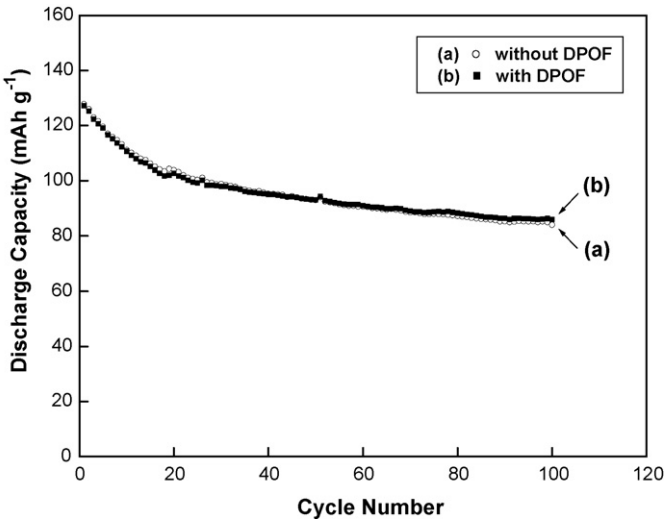

Fig. 5. Variations of discharge capacity with cycle number for Li-ion coin cells using an electrolyte consisting of 1.15 M $LiPF_6$/EC:EMC (3:7 vol.%) at 1*C* rate, RT (RT: room temperature).

ated with a structural change of $LiCoO_2$ and/or the formation of a solid electrolyte interface (SEI) film on the electrode surface [13].

In order to satisfy the demands of high-power applications, Li-ion cells must deliver good performances at high current drains. The variation in capacity at high rate can be explained by several processes in the cell, e.g., the electrical conductivity within the electrode, and diffusion and migration processes in the electrolyte [14]. The rate performances of cells under different discharge rates, namely, 0.2*C*, 0.5*C*, 1*C* and 2*C*, are given in Figs. 3 and 4. All the cells were charged with the CC/CV protocol at a rate of 0.2*C*. The rate performance of the cells is summarized in Table 3. In Fig. 3, both the capacity and voltage decrease with increasing discharge rate. This result can be explained in terms of electrode polarization due to an increased IR drop [15]. In Fig. 4 and Table 3, the cell with the DPOF-free electrolyte has a rate performance of 87% at a 2*C* rate. By contrast, the cell with the DPOF-containing electrolyte gives a good rate performance of 90% at a 2*C* rate.

The discharge capacity as a function of the cycle number for 100 cycles at room temperature is shown in Fig. 5. The electrochemical cycling test of the cells was carried out at a constant rate of 1*C* within a voltage range of 2.75–4.2 V. The cells with and without DPOF exhibit capacity retention of about 68% and 66% of the initial capacity after 100 cycles, respectively. This further confirms the improved cycling performance of the cell with DPOF. In addition, the discharge capacity of the cycled cell with DPOF (86.0 mAh g^{-1}) is higher than the DPOF-free cell (84.0 mAh g^{-1}) after 100 cycles. From these results, it is found that the presence of DPOF improves cycling performance.

Electrochemical impedance was measured during 100 cycles. The typical EIS result of the Li-ion cell and the equivalent circuit

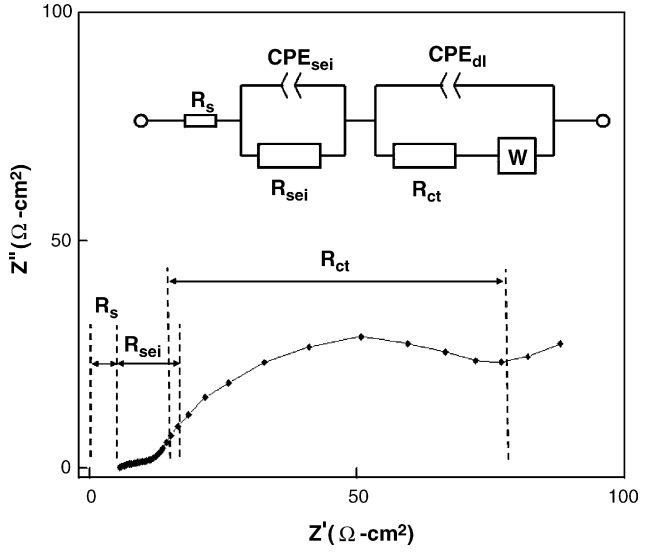

Fig. 6. Typical EIS of Li-ion cell and equivalent circuit used for the analyses of EIS.

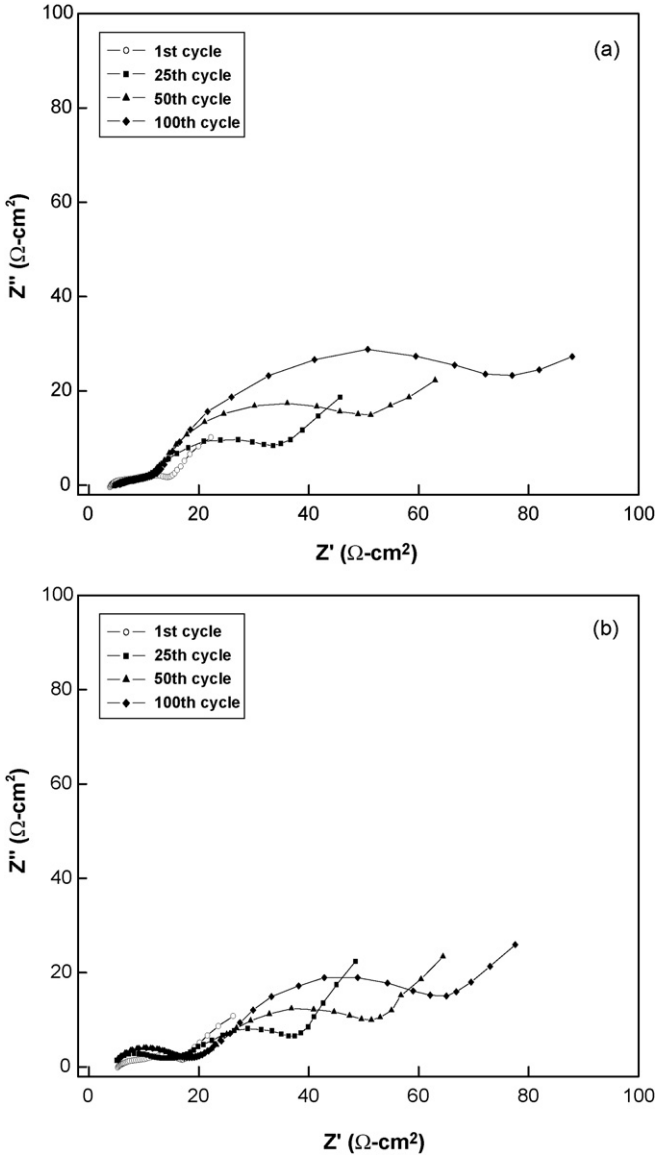

Fig. 7. Impedance plots of MCMB/$LiCoO_2$ cells using electrolytes consisting of 1.15 M $LiPF_6$/EC:EMC (3:7 vol.%) during 100 cycling at RT: (a) without DPOF; (b) with DPOF.

used for the EIS analysis are shown in Fig. 6. The EIS of the Li-ion cell is composed of two partially overlapping semi-circles and a straight sloping line at the low frequency end [16]. In Fig. 6, R_s is the cell electrolyte resistance, while R_{sei} and C_{sei} are the resistance and capacitance, respectively, of the SEI film formed on the surface of the electrodes, and correspond to the semi-circle at high frequencies. R_{ct} and C_{dl} are the charge-transfer resistance and the double-layer capacitance, respectively, which correspond to the semi-circle at medium frequencies. W is the Warburg impedance related to the effect of the diffusion of lithium ions at the electrode/electrolyte interface, which corresponds to the straight sloping line at the low-frequency end. Since R_s and R_{sei} are ohmic characteristics, their combination is referred to as the 'ohmic impedance'. The combination of R_{ct} and W is called the 'faradic impedance', which reflects the kinetics of the cell reactions [16–19]. Ning et al. reported that the impedance of the cell in the fully charged state is always lower than that in the fully discharged state [20].

The impedance curves measured after charging (4.2 V) at a 1C rate during 100 cycles of the MCMB/$LiCoO_2$ cells are shown in Fig. 7. The fitted values of R_s, R_{sei}, R_{ct} and R_{cell} are plotted as a function of the cycle number in Fig. 8. A comparison of the parameters is given in Table 4. Zhang et al. [19] reported that the total resistance (R_{cell}) of Li-ion cells is mainly composed of the bulk resistance (R_b), the solid-state interface resistance (R_{sei}) and the charge-transfer resistance (R_{ct}). The R_{cell} value of the Li-ion cell is predominated by the R_{ct} value, which reflects the kinetics of the cell reactions [19]. As indicated in Figs. 7 and 8, the total resistance (R_{cell}), especially R_{ct}, shows a larger increase compared with R_s and R_{sei} during 100 cycles. Fig. 8(c) gives plots of R_{ct} against the cycle number, which are similar to those of R_{cell}. The R_{cell} of the cell with DPOF is higher than that of the cell without DPOF during the first 50 cycles, but lower (71.2 Ω cm^2) than that of the cell without DPOF (75.5 Ω cm^2) after 100 cycles, as shown in Table 4. A comparison of Figs. 5, 7 and 8 shows that the cell with DPOF has an increased discharge capacity and decreased impedance. Therefore, the results of the EIS analysis are similar to those of the cycling tests.

Table 4
Comparisons of parameters measured after charging at 1C rate

Cycle no.	E1, resistance (Ω cm^2)				E2, resistance (Ω cm^2)			
	R_s	R_{sei}	R_{ct}	R_{cell}	R_s	R_{sei}	R_{ct}	R_{cell}
1	3.9	3.2	5.6	12.7	5.2	3.4	7.2	15.8
25	4.4	14.6	9.6	28.6	2.3	17.2	13.6	33.1
50	4.3	12.3	30.8	47.4	3.5	15.1	34.4	53.0
100	4.6	13.8	57.1	75.5	3.5	15.7	52.0	71.2

In order to investigate the effect of the additive on the electrode morphology before and after 100 cycles at the 1C rate, SEM images of the MCMB electrode were obtained and are presented in Fig. 9. The image for an uncycled electrode is given in Fig. 9(a). When the cell is cycled under a high discharge rate, the internal temperature will rise quickly and the surface film on the carbon particles will rapidly become thicker [20]. The micrograph of the electrode cycled with DPOF (Fig. 9(c)) displays a very different structural shape compared with that of the electrode cycled without DPOF (Fig. 9(b)). The DPOF-containing

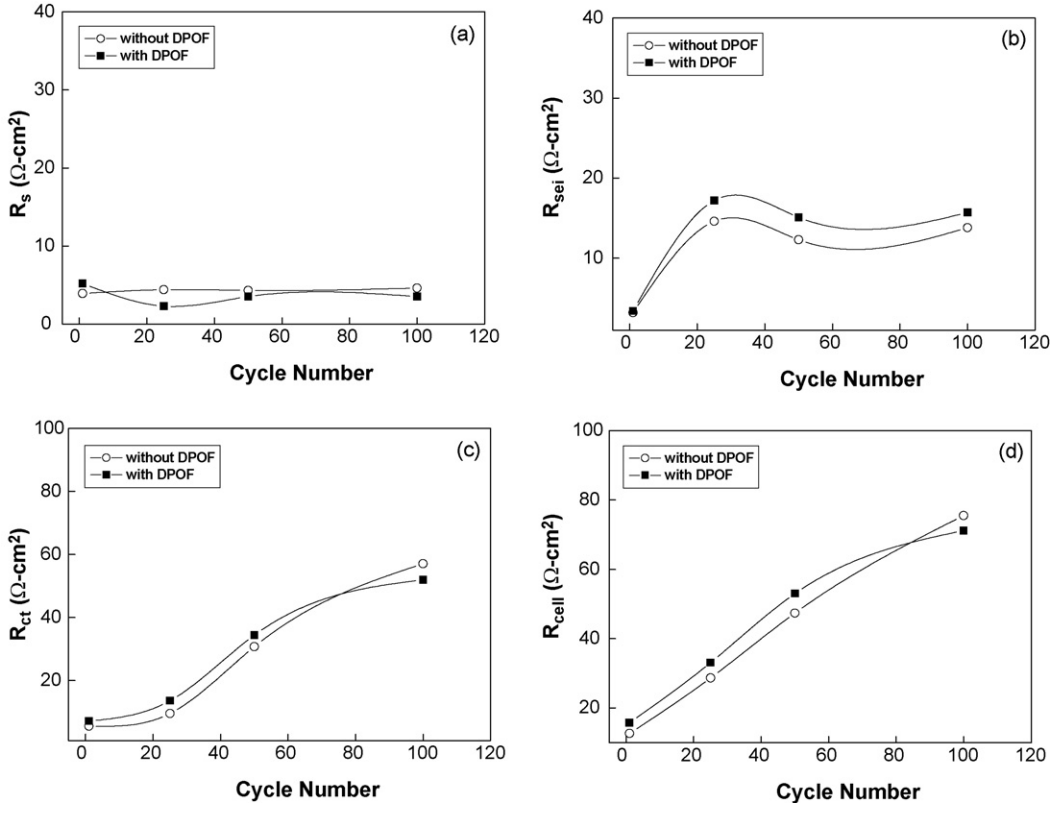

Fig. 8. The plots of R_s (a), R_{sei} (b), R_{ct} (c) and R_{cell} (d) measured after charging at 1C rate with the two electrolytes during 100 cycling at RT.

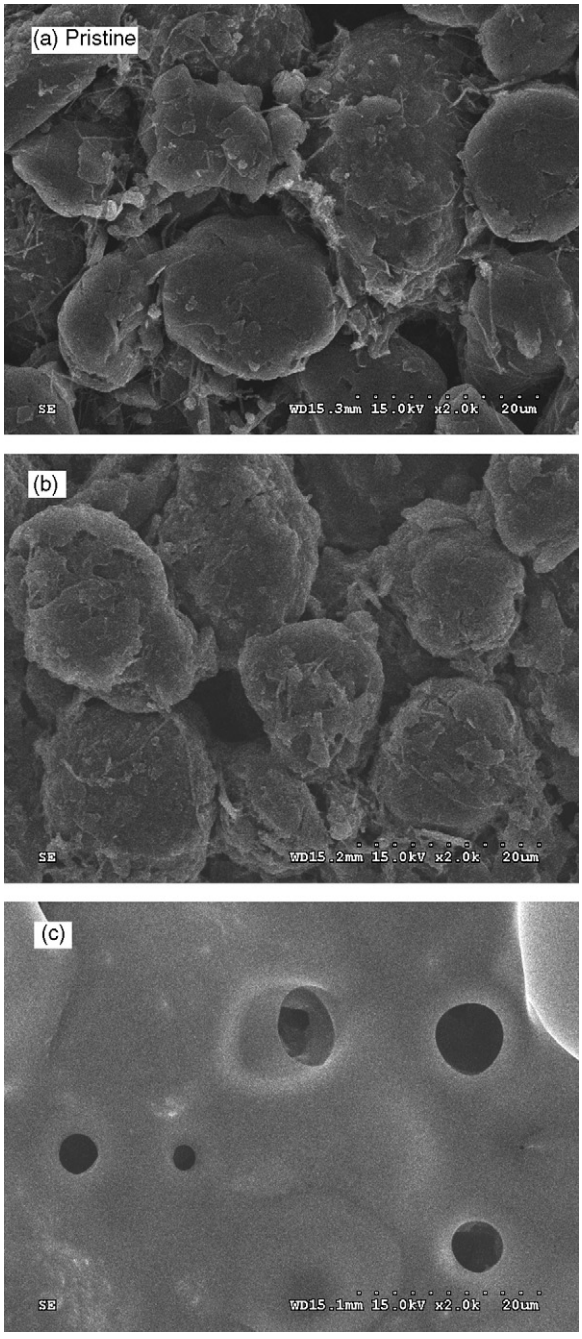

Fig. 9. SEM micrographs of MCMB electrodes before and after 100 cycles: (a) pristine electrode; (b) E1, without DPOF; (c) E2, with DPOF.

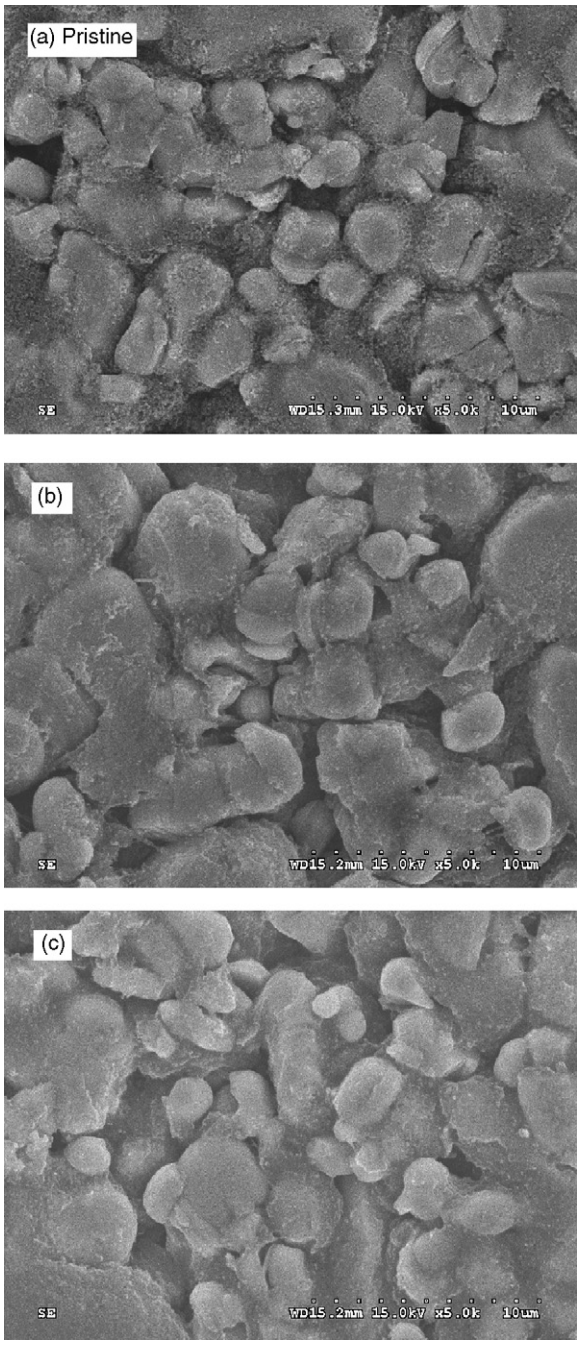

Fig. 10. SEM micrographs of $LiCoO_2$ electrodes before and after 100 cycles: (a) pristine electrode; (b) E1, without DPOF; (c) E2, with DPOF.

electrode is completely covered with a repeated layer of SEI film, due to the polymerization of the diphenyl. The layer is thicker than that on the DPOF-free electrode (Fig. 9(b)). It is assumed that the thick film is derived from the diphenyl [3,21,22] of the diphenyloctyl phosphate additive used in this work. Fig. 10 gives micrographs of the $LiCoO_2$ electrode with and without DPOF before and after 100 cycles. The electrode cycled with DPOF is covered with a thin and uniform film, which is significantly different from the thick surface film (Fig. 9(c)) on the anode.

In this study, it has been found that the addition of 5 wt.% DPOF as a flame-retardant additive in liquid electrolyte improves the cell performance and thermal stability of the electrolyte. These results confirm the efficacy of DPOF-containing electrolyte, due to the high reaction temperature and a decrease of the total resistance (R_{cell}), especially R_{ct}.

4. Conclusions

The influence of DPOF as a flame-retardant additive in a liquid electrolyte has been investigated. The DPOF-containing electrolyte is electrochemically stable up to about 4.95 V versus Li/Li^+. The thermal stability of the electrolyte is con-

siderably improved by the addition of 5 wt.% DPOF to a 1.15 M $LiPF_6$/EC:EMC (3:7 v/v) electrolyte. The cell with DPOF exhibits better electrochemical cell performance than that without DPOF, in both the initial charge/discharge and rate performance tests. In the cycling tests, a cell with the DPOF-containing electrolyte has a better discharge capacity and capacity retention than a cell with the DPOF-free electrolyte after cycling. This is confirmed because the total resistance of the cell, especially the charge-transfer resistance, is decreased after cycling. These results confirm the viability of using DPOF as a flame-retardant additive to improve the cell performance and the thermal stability of electrolytes for Li-ion batteries.

References

[1] J. Ma, C. Wang, S. Wroblewski, J. Power Sources 164 (2007) 849.
[2] Y. Hu, W. Kong, H. Li, X. Huang, L. Chen, Electrochem. Commun. 6 (2004) 126.
[3] L. Xiao, X. Ai, Y. Cao, H. Yang, Electrochim. Acta 49 (2004) 4189.
[4] H. Ota, A. Kominato, W.J. Chun, E. Yasukawa, S. Kasuya, J. Power Sources 119–121 (2003) 393.
[5] K. Xu, M.S. Ding, S. Zhang, J.L. Allen, T.R. Jow, J. Electrochem. Soc. 149 (2002) A622.
[6] X. Wang, E. Yasukawa, S. Kasuya, J. Electrochem. Soc. 148 (2001) A1058.
[7] S.I. Gonzales, W. Li, B.L. Lucht, J. Power Sources 135 (2004) 291.
[8] Q. Wang, J. Sun, C. Chen, J. Power Sources 162 (2006) 1363.
[9] S.S. Zhang, K. Xu, T.R. Jow, J. Power Sources 113 (2003) 166.
[10] K. Xu, M.S. Ding, S. Zhang, J.L. Allen, T.R. Jow, J. Electrochem. Soc. 150 (2003) A161.
[11] Y.E. Hyung, D.R. Vissers, K. Amine, J. Power Sources 119–121 (2003) 383.
[12] R.M. Millan, H. Slegr, Z.X. Shu, W. Wang, J. Power Sources 81–82 (1999) 20.
[13] M. Itagaki, N. Kobari, S. Yotsuda, K. Watanabe, S. Kinoshita, M. Ue, J. Power Sources 148 (2005) 78.
[14] J. Shim, R. Kostecki, T. Richardson, X. Song, K.A. Striebel, J. Power Sources 112 (2002) 222.
[15] S.S. Zhang, K. Xu, T.R. Jow, J. Power Sources 140 (2005) 361.
[16] S.S. Zhang, J. Power Sources 163 (2007) 713.
[17] S. Yang, H. Song, X. Chen, Electrochem. Commun. 8 (2006) 137.
[18] M. Itagaki, N. Kobari, S. Yotsuda, K. Watanabe, S. Kinoshita, M. Ue, J. Power Sources 135 (2004) 255.
[19] S.S. Zhang, K. Xu, T.R. Jow, Electrochim. Acta 49 (2004) 1057.
[20] G. Ning, B. Haran, B.N. Popov, J. Power Sources 117 (2003) 160.
[21] K. Abe, Y. Ushigoe, H. Yoshitake, M. Yoshio, J. Power Sources 153 (2006) 328.
[22] K. Shima, K. Shizuka, M. Ue, H. Ota, T. hatozaki, J.I. Yamaki, J. Power Sources 161 (2006) 1264.